Supplementary Data Guide

Inflammasome adaptor ASC suppresses apoptosis of gastric cancer cells by an IL-18 mediated inflammation-independent mechanism

Virginie Deswaerte, Paul Nguyen, Alison West, Alison F. Browning, Liang Yu, Saleela M. Ruwanpura, Jesse Balic, Thaleia Livis, Charlotte Girard, Adele Preaudet, Hiroko Oshima, Ka Yee Fung, Hazel Tye, Meri Najdovska, Matthias Ernst, Masanobu Oshima, Cem Gabay, Tracy Putoczki, Brendan J. Jenkins.

but no change in proliferation or infiltration of inflammatory cells, in the tumor epithelium of *gp130*$^{F/F}$ mice lacking IL-18.

Supplementary Figure S7. Genetic disruption of IL-18 in *gp130*$^{F/F}$ mice, whose augmented gene expression is observed in the gastric tumor epithelium of *gp130*$^{F/F}$ mice, does not interfere with the expression of cell cycle, angiogenesis or inflammatory genes.

Supplementary Figure S8. Caspase-1 preferentially processes mature IL-18 production and promotes growth in human gastric cancer cells.

Supplementary Table S1. Clinicopathological features and demographics of gastric cancer patients used for expression profiling of inflammasome-related components.

	Chinese cohort	**TCGA cohort[1]**
Mean age		
Years (range)	62 (35-88)	65.6 (50.4-81.3)
Sex [number (%)]		
Male	15 (63)	15 (83)
Female	7 (29)	3 (17)
Unknown	2 (8)	0 (0)
Histological type [number (%)]		
Intestinal-type	24 (100)	18 (100)
Diffuse	0 (0)	0 (0)
***Helicobacter pylori* status [number (%)]**		
Positive	8 (33)	1 (6)
Negative	13 (54)	4 (22)
Unknown	3 (13)	13 (72)
Tumor grade [number (%)]		
1	1 (4)	0 (0)
2	3 (13)	10 (56)
3	10 (42)	8 (44)
4	2 (8)	0 (0)
Unknown	8 (33)	0 (0)

[1]TCGA, The Cancer Genome Atlas

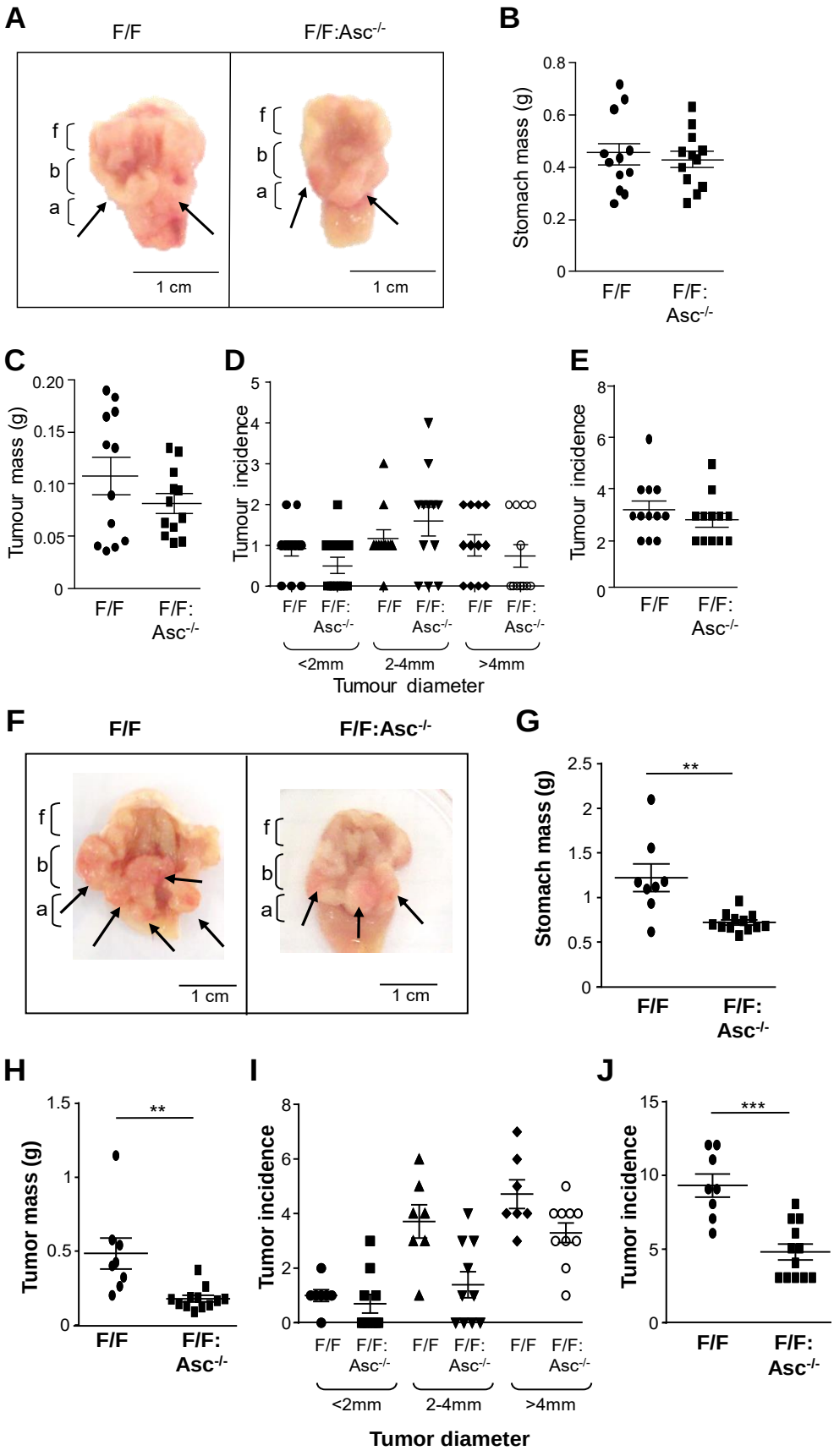
A
F/F
F/F:Asc-/-
f
b
a
1 cm
1 cm
B
Stomach mass (g)
0.8
0.6
0.4
0.2
0
F/F
F/F: Asc-/-
C
Tumour mass (g)
0.20
0.15
0.10
0.05
0
F/F
F/F: Asc-/-
D
Tumour incidence
5
4
3
2
1
0
F/F
F/F: Asc-/-
<2mm
2-4mm
>4mm
Tumour diameter
E
Tumour incidence
8
6
4
2
0
F/F
F/F: Asc-/-
F
F/F
F/F:Asc-/-
f
b
a
1 cm
1 cm
G
Stomach mass (g)
**
2.5
2
1.5
1
0.5
0
F/F
F/F: Asc-/-
H
Tumor mass (g)
**
1.5
1
0.5
0
F/F
F/F: Asc-/-
I
Tumor incidence
8
6
4
2
0
F/F
F/F: Asc-/-
<2mm
2-4mm
>4mm
Tumor diameter
J
Tumor incidence
***
15
10
5
0
F/F
F/F: Asc-/-

Supplementary Figure S1. Gastric tumor formation in 10-12 and 30-34 week old *gp130*$^{F/F}$ mice lacking ASC. (A) Representative appearance of stomachs from 10-12 week old (wo) *gp130*$^{F/F}$ (F/F) and *gp130*$^{F/F}$:*Asc*$^{-/-}$ (F/F:Asc$^{-/-}$) mice (shown is 1 out of 12 representative stomach image/genotype). Arrows indicate macroscopically visible tumors. Fundic (f), body (b) and antral (a) stomach regions are depicted. (B-E) Scatter plots depicting the total mass (grams; g) of stomachs (B) and gastric tumors (C), as well as the incidence of tumors by size (D) and in total (E), from F/F and F/F:Asc$^{-/-}$ 10-12wo mice. (F-J) Same layout of data as in (A-E), except for 30-34wo F/F and F/F:Asc$^{-/-}$ mice. Data for each genotype are expressed as the mean ± SEM. $^{**}P < 0.01$, $^{***}P < 0.001$; unpaired t-test.

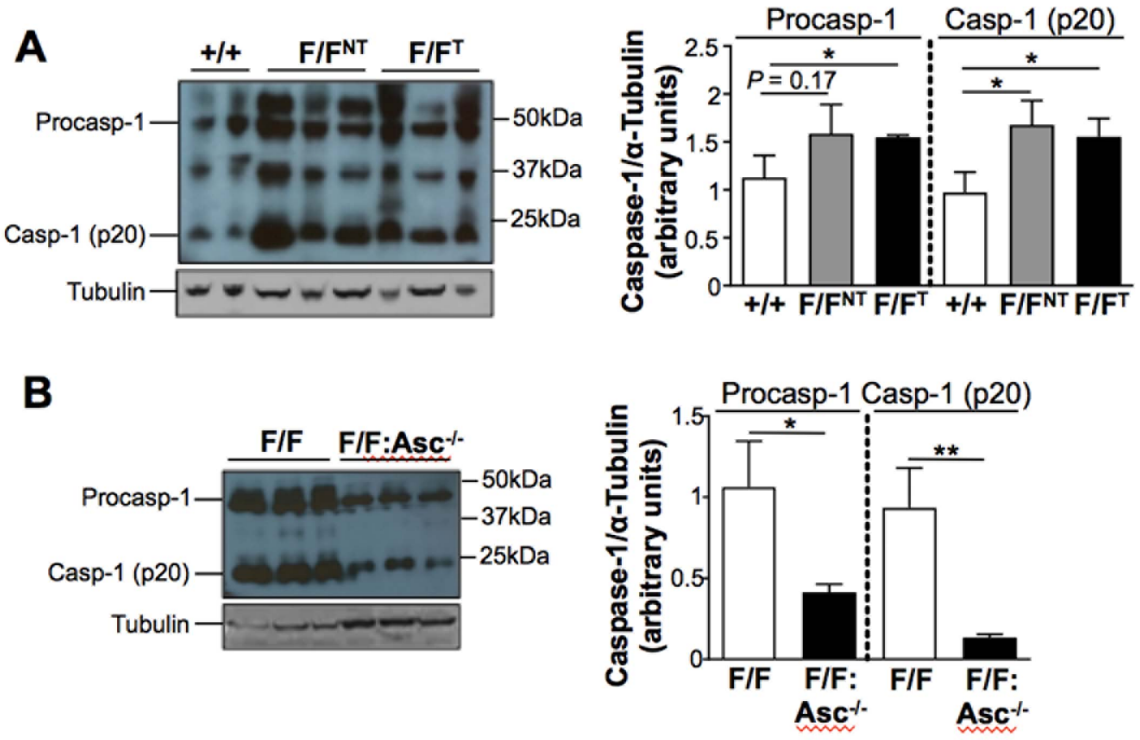

Supplementary Figure S2. Genetic disruption of ASC in *gp130*$^{F/F}$ mice suppresses activation of caspase-1. (A) Immunoblots and quantification graphs (n = 5/genotype) of gastric antral tissue lysates from 20-24 week old (wo) *gp130*$^{+/+}$ (+/+) and *gp130*$^{F/F}$ (F/F) mice with the indicated antibodies. NT, non-tumor; T, tumor. (B) Immunoblots and quantification graphs (n = 6/genotype) of gastric tumor lysates from 20-24wo F/F and *gp130*$^{F/F}$:*Asc*$^{-/-}$ (F/F:Asc$^{-/-}$) mice with the indicated antibodies. In both (A) and (B), each lane represents an individual mouse sample. Data for each genotype are expressed as the mean ± SEM. **P* < 0.05, ***P* < 0.01; unpaired t-test.

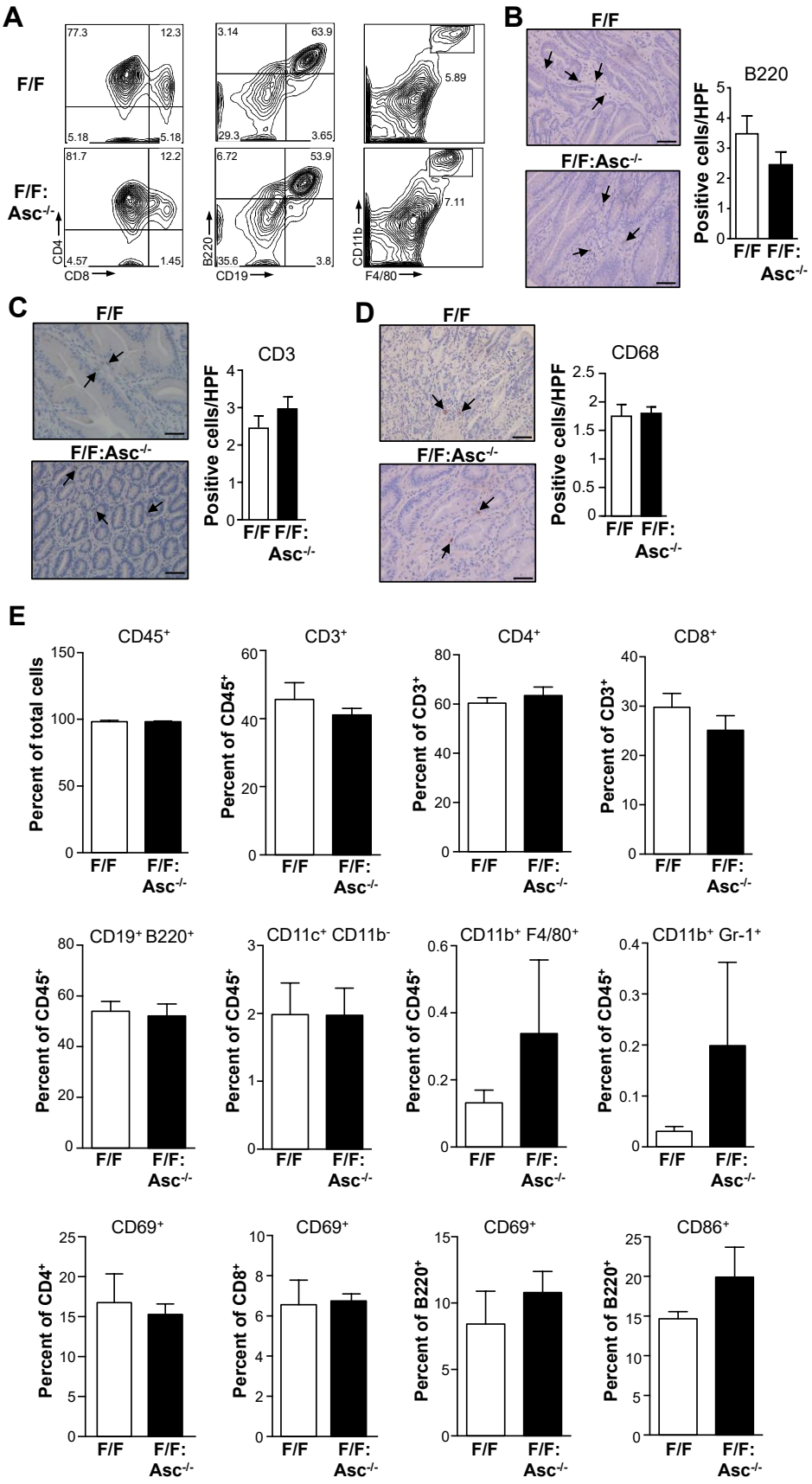
A
F/F
F/F:Asc-/-
77.3
12.3
5.18
5.18
81.7
12.2
4.57
1.45
CD4
CD8
3.14
63.9
29.3
3.65
6.72
53.9
35.6
3.8
B220
CD19
5.89
7.11
CD11b
F4/80
B
F/F
F/F:Asc-/-
B220
Positive cells/HPF
F/F
F/F: Asc-/-
C
F/F
F/F:Asc-/-
CD3
Positive cells/HPF
F/F
F/F: Asc-/-
D
F/F
F/F:Asc-/-
CD68
Positive cells/HPF
F/F
F/F: Asc-/-
E
CD45+
Percent of total cells
CD3+
Percent of CD45+
CD4+
Percent of CD3+
CD8+
Percent of CD3+
CD19+ B220+
Percent of CD45+
CD11c+ CD11b-
Percent of CD45+
CD11b+ F4/80+
Percent of CD45+
CD11b+ Gr-1+
Percent of CD45+
CD69+
Percent of CD4+
CD69+
Percent of CD8+
CD69+
Percent of B220+
CD86+
Percent of B220+
F/F
F/F: Asc-/-

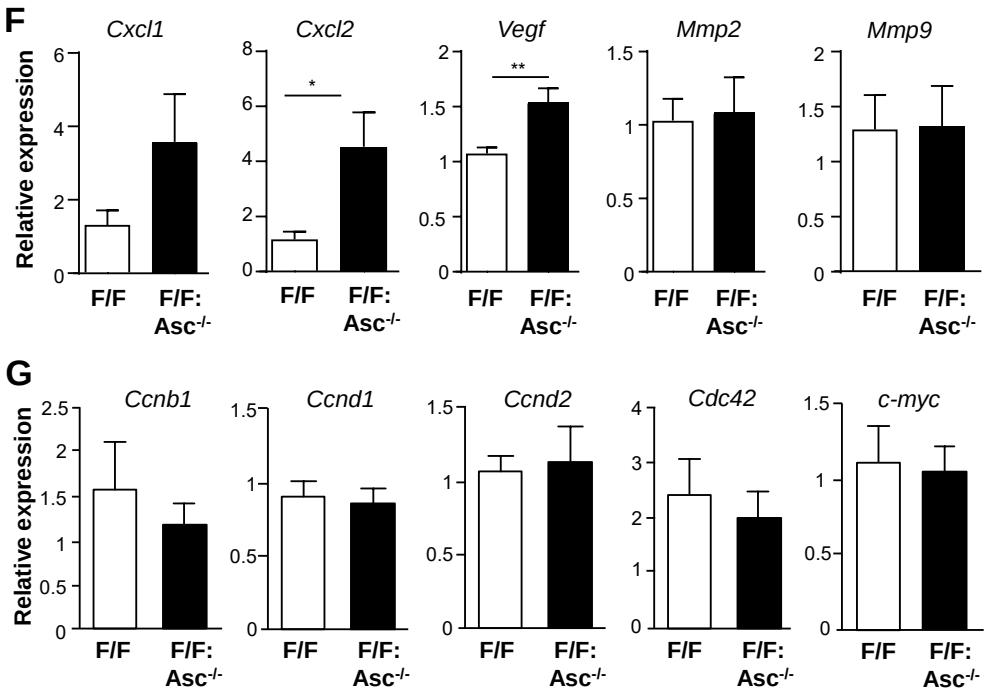

Supplementary Figure S3. Genetic disruption of ASC does not suppress gastric inflammation in *gp130*$^{F/F}$ mice, nor expression of angiogenic or cell cycle genes. (A) Representative flow cytometry plots showing the proportion of cells positive for CD4/CD8, B220/CD19 and CD11b/F4/80 in the stomachs of *gp130*$^{F/F}$ (F/F) and *gp130*$^{F/F}$:*Asc*$^{-/-}$ (F/F:Asc$^{-/-}$) 20-24 week old (wo) mice (shown is 1 out of 6 representative plot/genotype). Numbers indicate frequency of the gated population. (B-D) Representative B220-stained (B), CD3-stained (C) and CD68-stained (D) cross-sections through the antral tumor region of 20-24wo F/F and F/F:Asc$^{-/-}$ mouse stomachs (shown is 1 out of 8 representative image/genotype). Positive cells are depicted by arrows. Scale bars: 50µm. Graphs depict quantitative enumeration of positive cells per high power (40x) field (HPF) in the gastric tumor mucosa from the indicated mice. Data are presented as the mean ± SEM from n = 8 mice/genotype. (E) Graphs depicting the frequencies of the indicated cell populations in

the perigastric lymph nodes of F/F and F/F:Asc$^{-/-}$ 20-24wo mice (n = 4/genotype) as determined by flow cytometry. Data are presented as the mean ± SEM. (F and G) qPCR expression analyses of angiogenic genes (F) and cell cycle genes (G) in antral gastric tumor tissue of 20-24wo F/F or F/F:Asc$^{-/-}$ mice (n = 8/genotype). Expression data are shown following normalization for *18S rRNA*, and are presented from experimental triplicates as the mean ± SEM. *$P < 0.05$, **$P < 0.01$; unpaired t-test.

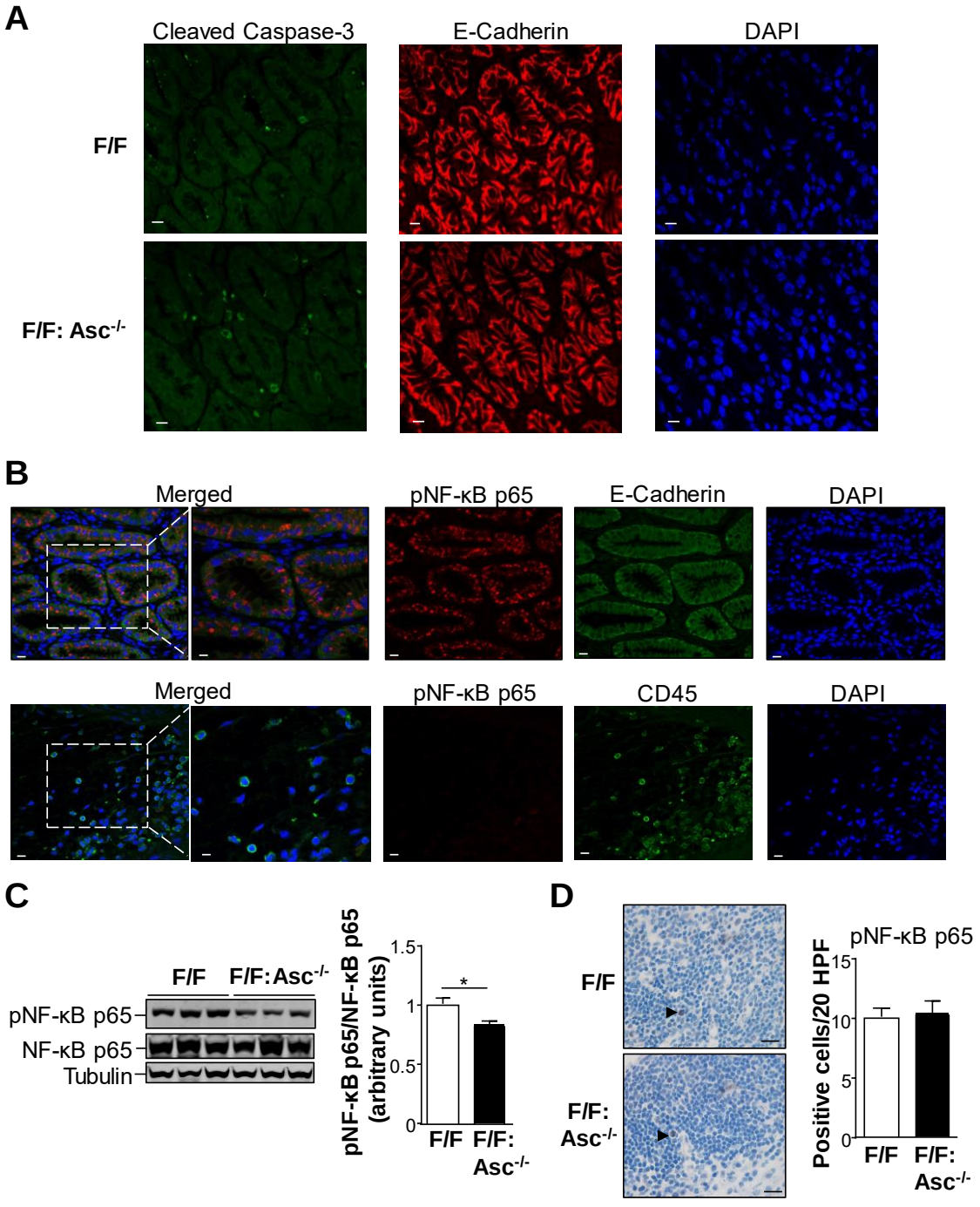

Supplementary Figure S4. Elevated apoptotic epithelial cell numbers and reduced NF-κB activation in gastric tumors of *gp130*$^{F/F}$ mice lacking ASC. (A) Representative confocal

immunofluorescence photomicrographs of cells stained for cleaved caspase-3 (green), E-cadherin (red, epithelial cell marker) or the nuclear marker 4',6-diamidino-2-phenylindole (DAPI; blue) alone in cross-sections of gastric tumor tissues from 6 month old (mo) *gp130*$^{F/F}$ (F/F) and *gp130*$^{F/F}$:*Asc*$^{-/-}$ (F/F:Asc$^{-/-}$) mice. Scale bars: 40μm. (B) Representative confocal immunofluorescence photomicrographs of cells stained for cleaved E-cadherin (green; upper panels), CD45 (green, immune cell marker, lower panels), pNF-κB p65 (red) or DAPI (blue) either alone or merged in cross-sections of gastric tumor mucosal (upper panels) and submucosal (lower panels) regions from 6mo F/F mice. Scale bars: 40μm for low power images, and 25μm for high power images (second merged image from the left). (C) Immunoblots and quantification graph (n = 8/genotype) of gastric tumor lysates from 20-24wo F/F and F/F:Asc$^{-/-}$ mice with the indicated antibodies. Each lane represents an individual mouse sample. ***$P < 0.001$; unpaired t-test. (D) Representative pNF-κB p65-stained cross-sections through the submucosal region of tumor-bearing 20-24wo F/F and F/F:Asc$^{-/-}$ mouse stomachs (shown is 1 out of 6 representative image/genotype). Scale bars: 50μm. Graph depicting the percentage of pNF-κB p65 positive cells/area in the gastric tumor mucosa from mice of the indicated genotypes. Data for each genotype (n = 6) are expressed as the mean ± SEM. **$P < 0.01$; unpaired t-test.

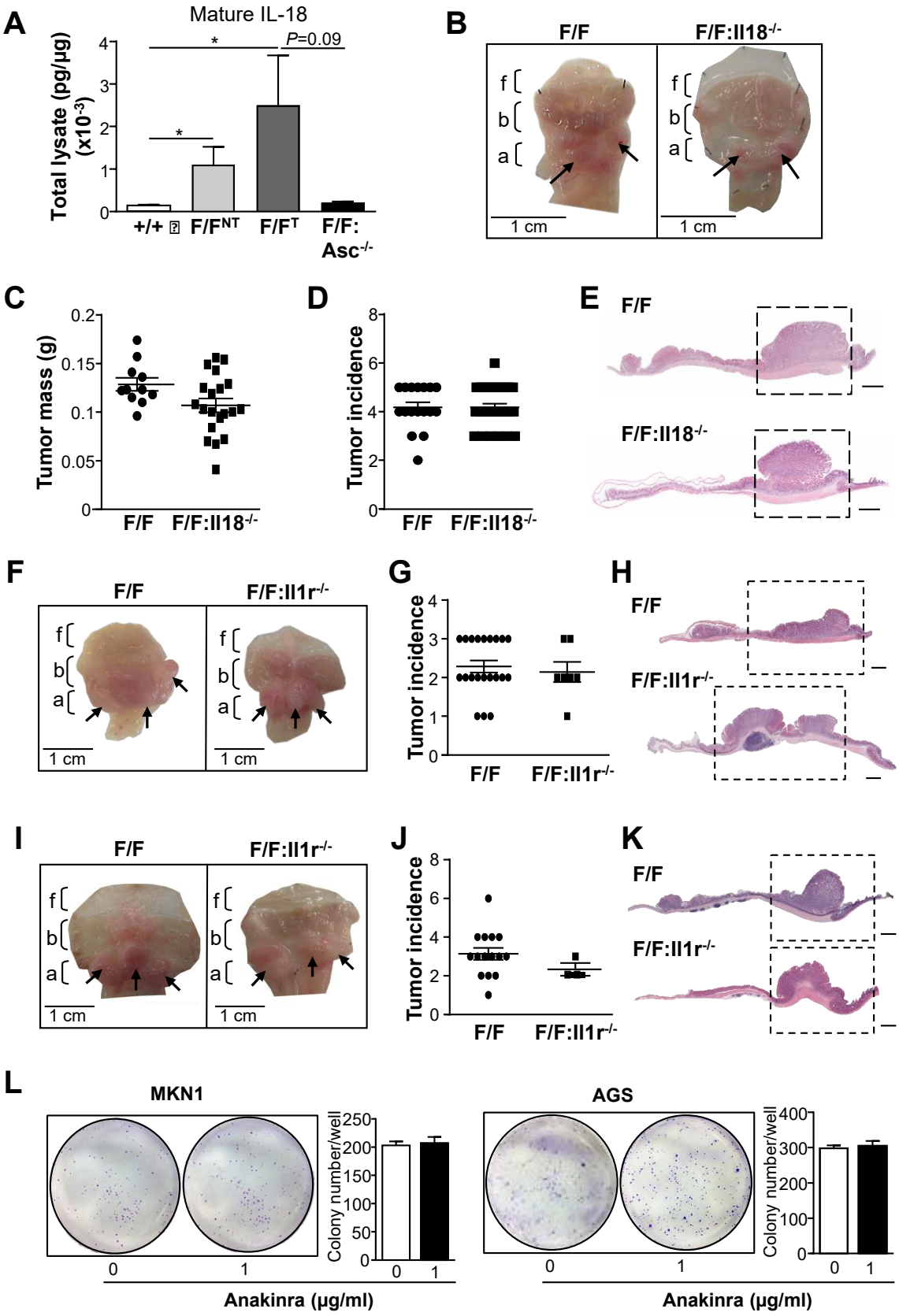
A
Mature IL-18
Total lysate (pg/µg) (x10-3)
*
P=0.09
*
+/+
F/FNT
F/FT
F/F: Asc-/-
B
F/F
F/F:Il18-/-
f
b
a
1 cm
C
Tumor mass (g)
F/F
F/F:Il18-/-
D
Tumor incidence
F/F
F/F:Il18-/-
E
F/F
F/F:Il18-/-
F
F/F
F/F:Il1r-/-
1 cm
G
Tumor incidence
F/F
F/F:Il1r-/-
H
F/F
F/F:Il1r-/-
I
F/F
F/F:Il1r-/-
1 cm
J
Tumor incidence
F/F
F/F:Il1r-/-
K
F/F
F/F:Il1r-/-
L
MKN1
Colony number/well
Anakinra (µg/ml)
AGS
Colony number/well
Anakinra (µg/ml)

Supplementary Figure S5. Gastric tumor formation is unaltered in 10-12 week old *gp130*$^{F/F}$ mice lacking IL-18, or upon genetic disruption of the IL-1R in *gp130*$^{F/F}$ mice. (A) ELISA for mature IL-18 protein in antral gastric tissue from 20-24wo *gp130*$^{+/+}$ (+/+) mice, and tumor (T) and non-tumor (NT) tissue from age-matched *gp130*$^{F/F}$ (F/F) or *gp130*$^{F/F}$:*Asc*$^{-/-}$ (F/F:Asc$^{-/-}$) mice. Data are presented as the mean ± SEM (n = 4-6 mice per group). **P* < 0.05; unpaired t-test. (B) Representative appearance of stomachs from 10-12 week old (wo) *gp130*$^{F/F}$ (F/F) and *gp130*$^{F/F}$:*Il18*$^{-/-}$ (F/F:Il18$^{-/-}$) mice (shown is 1 out of 11-20 representative stomach image/genotype). Arrows indicate macroscopically visible tumors. Fundic (f), body (b) and antral (a) stomach regions are depicted. (C and D) Scatter plots depicting the total mass (grams; g) of gastric tumors (C), and the total incidence of tumors (D), from F/F and F/F:Il18$^{-/-}$ 10-12wo mice. Data for each genotype are expressed as the mean ± SEM. **(**E) Representative photomicrographs showing H&E-stained whole stomach cross-sections from 10-12wo mice of the indicated genotypes (shown is 1 out of 11-20 representative stomach image/genotype). Adenomatous polyps (tumors) are depicted by the dotted square. Scale bars: 1mm. (F and I) Representative appearance of stomachs from 10-12wo (F) and 20-24wo (I) *gp130*$^{F/F}$ (F/F) and *gp130*$^{F/F}$:*Il1r*$^{-/-}$ (F/F:Il1r$^{-/-}$) mice (shown is 1 out of 7-21 (10-12wo) and 1 out of 5-15 (20-24wo) representative stomach image/genotype). Arrows indicate macroscopically visible tumors. Fundic (f), body (b) and antral (a) stomach regions are depicted. (G and J) Scatter plots depicting the total incidence of tumors from F/F and F/F:Il1r$^{-/-}$ 10-12wo (G) and 20-24wo (J) mice. Data for each genotype are expressed as the mean ± SEM. (H and K) Representative photomicrographs showing H&E-stained whole stomach cross-sections from 10-12wo (H) and 20-24wo (K) mice of the indicated genotypes (shown is 1 out of 7-21 (10-12wo) and 1 out of 5-15 (20-24wo)

representative stomach image/genotype). Adenomatous polyps (tumors) are depicted by the dotted squares. Scale bars: 1mm. (L) Anakinra treatment of human gastric cancer cells has no effect on colony formation. Representative images showing colony formation of human MKN1 and AGS cells treated with anakinra (shown is 1 out of 4-6 representative wells/treatment group per experiment). The number of colonies/well are expressed as the mean ± SEM from 3 separate experiments.

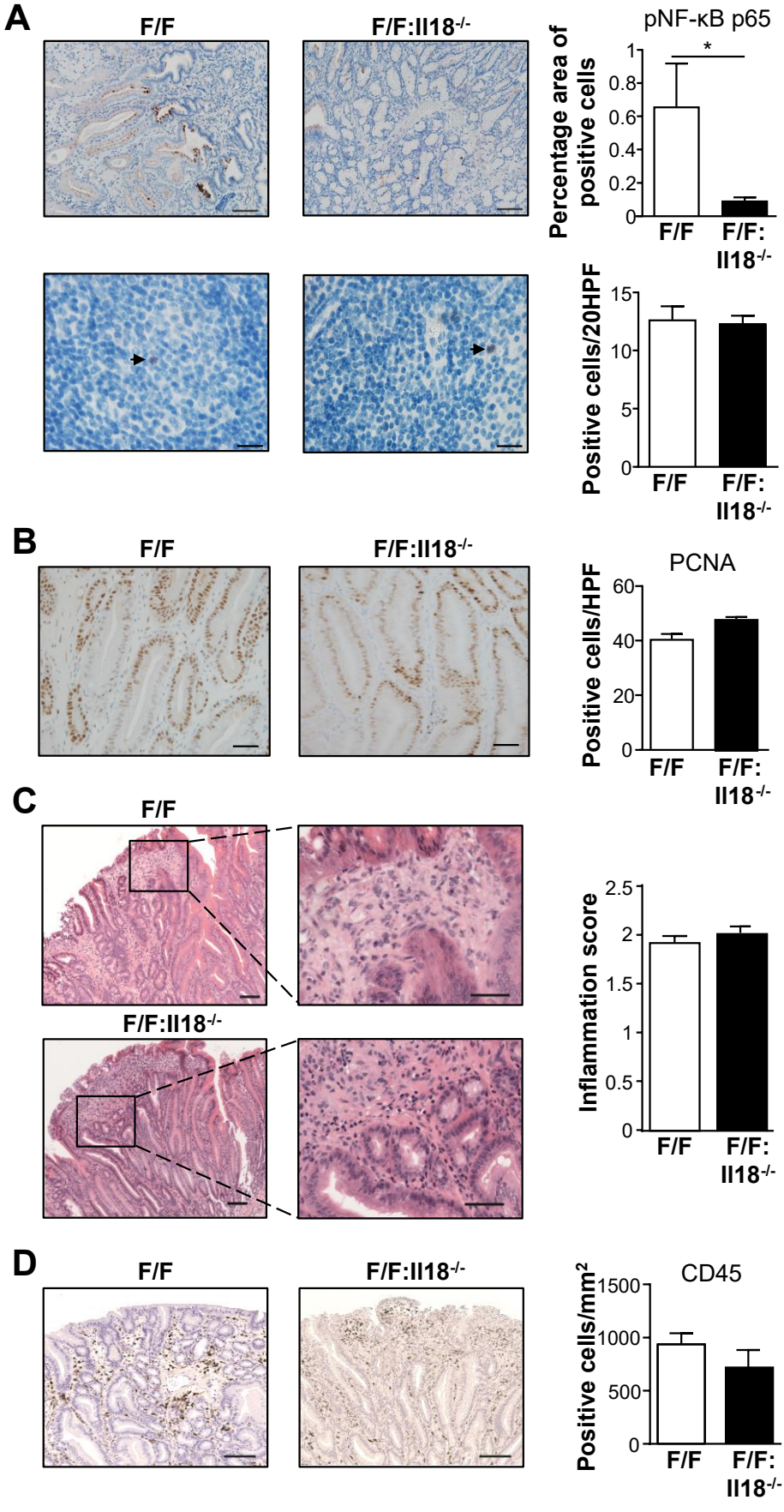
A
F/F
F/F:Il18-/-
pNF-κB p65
Percentage area of positive cells
1
0.8
0.6
0.4
0.2
0
*
F/F
F/F: Il18-/-
Positive cells/20HPF
15
10
5
0
F/F
F/F: Il18-/-
B
F/F
F/F:Il18-/-
PCNA
Positive cells/HPF
60
40
20
0
F/F
F/F: Il18-/-
C
F/F
F/F:Il18-/-
Inflammation score
2.5
2
1.5
1
0.5
0
F/F
F/F: Il18-/-
D
F/F
F/F:Il18-/-
CD45
Positive cells/mm2
1500
1000
500
0
F/F
F/F: Il18-/-

Supplementary Figure S6. Decrease of apoptotic and pNF-κB-expressing cell numbers, but no change in proliferation or infiltration of inflammatory cells, in the tumor epithelium of *gp130*$^{F/F}$ mice lacking IL-18. (A) Representative pNF-κB p65-stained cross-sections through the antral tumor (upper panels) and submucosal (lower panels) regions of 20-24 week old (wo) *gp130*$^{F/F}$ (F/F) and *gp130*$^{F/F}$:*Il18*$^{-/-}$ (F/F:Il18$^{-/-}$) mouse stomachs (shown is 1 out of 6 representative image/genotype). Scale bars: 50μm. Graph depicting the percentage of pNF-κB p65-positive cells/area in the gastric tumor mucosa from mice of the indicated genotypes. (B) Representative photomicrographs showing PCNA-stained cross-sections through the antral tumor-bearing region of stomachs from 20-24wo F/F and F/F:Il18$^{-/-}$ mice. Scale bars: 50μm. Graph depicting quantitative enumeration of PCNA-positive cells per high power (40×) field (HPF) in the gastric tumor mucosa from mice. (C) Left panels: representative H&E-stained cross-sections through the antral tumor region of 20-24wo F/F and F/F:Il18$^{-/-}$ mouse stomachs. Scale bar: 50μm. Right panels; magnified areas demonstrating the presence of inflammatory cell infiltrates in the mucosal epithelium. Scale bar: 20μm. Graph depicting inflammatory scores, based on 0-3 (none, mild, moderate, severe) scoring, from n = 6 mice/genotype. (D) Representative CD45-stained cross-sections through the antral tumor region of 20-24wo F/F and F/F:Il18$^{-/-}$ mouse stomachs. Scale bar: 50μm. Graph depicting quantitative enumeration of CD45-positive cells per mm^2 area in the gastric tumor mucosa from mice of the indicated genotypes. In (A-D), shown is 1 out of 6 representative image/genotype, and the data in graphs for each genotype (n = 6) are expressed as the mean ± SEM. *P < 0.05; unpaired t-test.

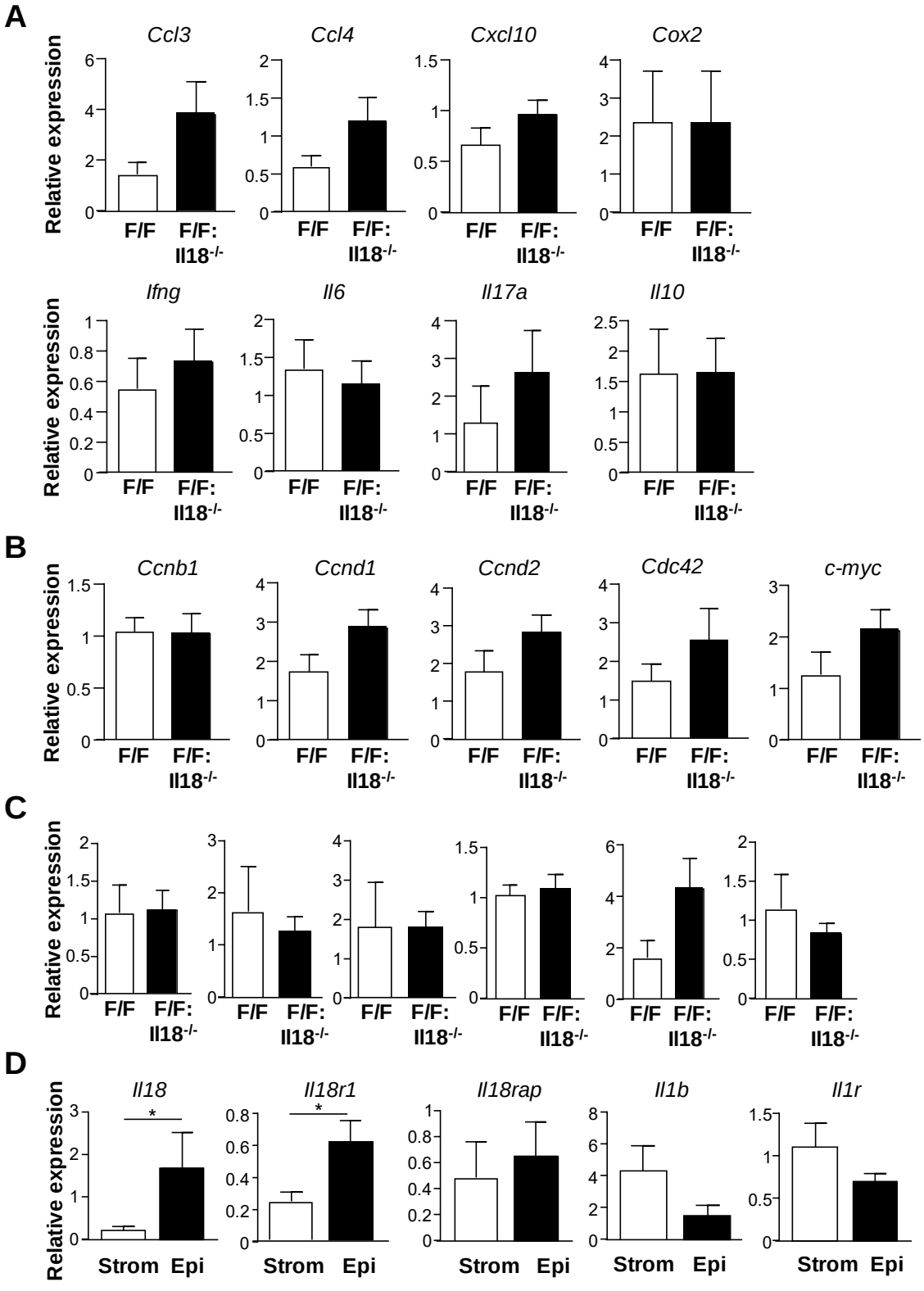
A
Ccl3
Ccl4
Cxcl10
Cox2
Ifng
Il6
Il17a
Il10
Relative expression
F/F
F/F: Il18-/-
B
Ccnb1
Ccnd1
Ccnd2
Cdc42
c-myc
C
D
Il18
Il18r1
Il18rap
Il1b
Il1r
Strom
Epi
*

Supplementary Figure S7. Genetic disruption of IL-18, whose augmented gene expression is observed in the gastric tumor epithelium of *gp130*$^{F/F}$ mice, does not interfere with the expression of cell cycle, angiogenesis or inflammatory genes. (A-C) qPCR expression analyses of the indicated inflammatory (A), cell cycle (B) and angiogenesis (C) genes in antral gastric tumor tissue of 20-24 week old (wo) *gp130*$^{F/F}$ (F/F) or *gp130*$^{F/F}$:*Il18*$^{-/-}$ (F/F:Il18$^{-/-}$) mice (n = 5/genotype). Expression data are shown following normalization for *18S rRNA*, and are presented from experimental triplicates as the mean ± SEM. (D) qPCR expression analyses of the indicated genes in captured laser microdissected gastric tumor epithelial (Epi) and stroma (Strom) tissue from 20-24wo F/F mice. Expression data from 5 samples/genotype are shown following normalization for *18S rRNA*, and are presented from technical triplicates as the mean ± SEM. **P* < 0.05; unpaired t-test.

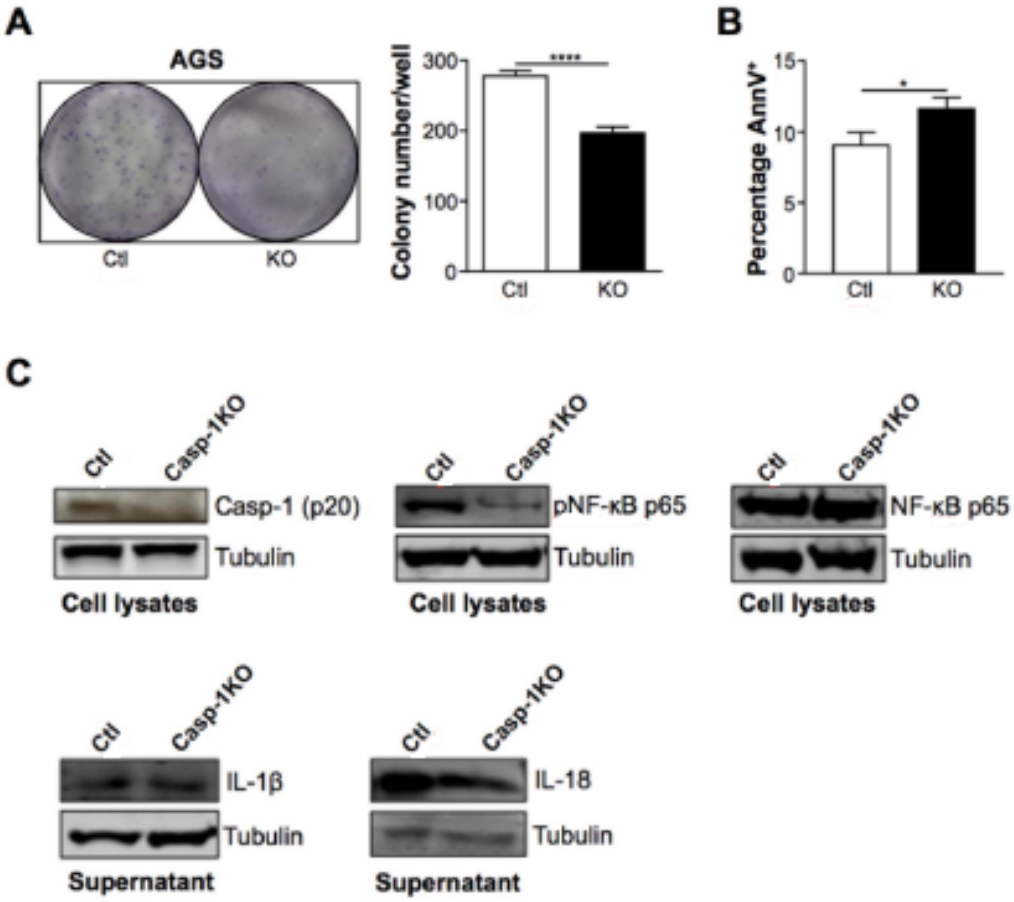

Supplementary Figure S8. Caspase-1 preferentially processes mature IL-18 production and promotes growth in human gastric cancer cells. (A) Representative images (1 of 6/group) showing colony formation of human AGS cells transduced with non-targeted control sgRNA (Ctl) and caspase-1 sgRNA (KO). Graph depicts colony number/well (6 wells/group) expressed as the mean ± SEM. ****$P < 0.0001$; unpaired t-test. (B) Flow cytometry of apoptotic Annexin-V-positive AGS Ctl and caspase-1 KO cells cultured for 24 hours. *$P < 0.05$; unpaired t-test. (C) Immunoblots with the indicated antibodies on cell culture supernatants and cell lysates from AGS Ctl and caspase-1 KO cells cultured for 24 hours.